

See discussions, stats, and author profiles for this publication at: <https://www.researchgate.net/publication/7295229>

Goldsmith, M. R. et al. The chiroptical signature of achiral metal clusters induced by dissymmetric adsorbates. *Phys. Chem. Chem. Phys.* 8, 63–67

ARTICLE *in* PHYSICAL CHEMISTRY CHEMICAL PHYSICS · FEBRUARY 2006

Impact Factor: 4.49 · DOI: 10.1039/b511563a · Source: PubMed

CITATIONS

57

READS

7

7 AUTHORS, INCLUDING:



Michael-Rock Goldsmith

United States Environmental Protection Ag...

45 PUBLICATIONS 428 CITATIONS

SEE PROFILE



Ron Naaman

Weizmann Institute of Science

304 PUBLICATIONS 5,290 CITATIONS

SEE PROFILE

The Chiroptical Signatures of Achiral Metal Clusters induced by Dissymmetric Adsorbates

Michael-Rock Goldsmith, Christopher B. George, Gerard Zuber, Ron Naaman, David H. Waldeck, Peter Wipf, David N. Beratan

Provided are details for the dissymmetrically-perturbed PIB method (Sections 1.1-1.3, pp S1-S4), nanoparticle structure-related information (Section 2.1.1, p S-5), the achiral perturbation test case (Section 2.1.2, p. S-5), an example of the *distance-dependent CD* and effect on chiral image charges by separating the adsorbates from the core (Section 2.1.3, p. S-6). In addition we list the Extended-Huckel calculations used to visualize chiral image-charges [1,2] (Section 2.2, p. S-7), and the *time-dependent resolution-of-identity approximation density functional theory* (TD-RI-DFT) method (Section 2.3, p.S-7) which uses the Random-Phase Approximation (RPA) single-excitation [10-15] approach to compute circular dichroism spectra of chiral-*monolayer protected clusters* (CMPCs) with both (a) explicit adsorbate and (b) coarse-grained point-charge adsorbate variations. The CPPIB model was built and developed using the gridMathematica software package.[7]

1.1 The Charge-Perturbed Particle-In-A-Box Model (CPPIB)

Applying the particle-in-a-box model (or the jellium model) to conducting metals or nanoparticles is not a novel theoretical endeavour and has been successfully applied in recent years to quantum dots, nano-wires of Au deposited on gold (Au) or Nickel (Ni) substrates, or Au nano-island defects on gold.[3-6] To the best of our knowledge, there exists no current theoretical interpretation of the induced rotational strengths incurred in an achiral metal nanocluster in the presence of chiral ligand or adsorbate, though it had been suggested by Whetten in consideration of the phenomena at hand. Hence, we introduce a simple PIB-based model that will enable us to explore the chiral-image-charges (CICs) as a result of a simplified interaction potential between the adlayer/adsorbate or monolayer molecules. We are able to visualize the induced CICs in the nanoparticle using this methodology, and more importantly we are able to make predictions towards the presence, parity and magnitude of the resultant chiroptic response of the chiral image charges; we introduce the concept of the chirally-perturbed particle-in-a-box model (CPPIB). There are several assumptions used in developing this model that need to be addressed:

- 1) the gold nanoparticle core of CMPCs are minimally distorted, and hence remain close to their bulk lattice constant, and perhaps more importantly, remain achiral.
- 2) The basis set describing the n-particle box is composed of combinations of ground-state PIB wave-functions, which are mathematically exact analytical expressions. The number of particle or electrons to consider is directly related to the number of Au atoms comprising the metal core, under the assumption that each Au atom contributes only its $6S^1$ conducting electrons.
- 3) the admolecules that interact directly with the gold core are coarse-grained to point-charge systems with nuclear coordinates of the admolecules (derived from a separate set of EHT semiempirical calculations).
- 4) the only interaction between (2) the admolecules and (1) the core occurs via an internal (to the box) perturbation which is exactly described by the Coulombic electrostatic potential function (between the exterior charges and the PIB wavefunctions).
- 5) The perturbation (4) is "permitted" to interact with the box to first order, and is solved using perturbation theory to obtain a set of perturbed PIB state functions comprised of linear combinations of unperturbed wavefunctions with 1st-order perturbation wavefunction coefficients.

The CPPIB model, as any PIB model, is based upon several well-known analytic expressions, for which the unperturbed or ground state is known exactly. The basis functions of the CPPIB model, both perturbed and unperturbed are expressed as:

$$\begin{aligned}\psi_{(x,y,z)}^0 &= \sqrt{\frac{8}{a \cdot b \cdot c}} \sin\left(\frac{n_x x}{a}\right) \sin\left(\frac{n_y y}{b}\right) \sin\left(\frac{n_z z}{c}\right) \\ E_{k_n} &= \frac{h^2}{8m} (k_n^2) \\ k_n &= \left(\frac{n_x^2}{a^2}\right) + \left(\frac{n_y^2}{b^2}\right) + \left(\frac{n_z^2}{c^2}\right) \quad k = (n_x, n_y, n_z) \dots N \\ n_x, n_y, n_z &= 1, 2, 3, \dots, N\end{aligned}$$

where the k^{th} state is made up of combinations of the three index quantum numbers n_x , n_y and n_z , and the energies of each k^{th} state apply, in this case, only to the unperturbed CPPIB model. The unperturbed Hamiltonian \hat{H}^0 , used to obtain these well-known expressions is typically applied in the context;

$$\hat{H}^0 \psi_{ij} = \int_0^a \int_0^b \int_0^c \psi_i^0 \hat{H}^0 \psi_{x,y,z}^0 dx dy dz$$

and solving the secular determinant allows us to obtain the eigenstates and eigenvalues of the PIB wavefunction. However, since the PIB state solutions are known, the energies of the k^{th} states, E_{k_n} , are used as the diagonal terms of the T matrix.

$$T^0 = \begin{bmatrix} E_{k_1} & 0 & 0 & 0 \\ 0 & E_{k_2} & 0 & 0 \\ 0 & 0 & \dots & 0 \\ 0 & 0 & 0 & E_{k_n} \end{bmatrix}$$

1.2. The Chiral Charge Perturbation Term: \hat{V}

In addition to the unperturbed Hamiltonian (the T^0 matrix), we require a V matrix, in our case the external chiral perturbation, which will allow us to conceivably formulate the total Hamiltonian as a sum of the unperturbed ground state T_{ii}^0 elements with the perturbation \hat{V} matrix elements.

Under no external perturbation the criteria for the internal and external potential of the CPPIB are those of the PIB model, namely:

$$\hat{V}^0 = \begin{cases} 0 & \text{if } 0 < x < a, 0 < y < b, 0 < z < c \\ \infty & \text{if } 0 \geq x \geq a, 0 \geq y \geq b, 0 \geq z \geq c \end{cases}$$

Since the perturbation expansion is problematic for states lying very close in energy, as in the PIB case, we will continue our formulation using degenerate time-independent perturbation theory. We introduce an external molecular perturbation outside the box. This effectively is a coarse-grained adsorbate represented as EHT-derived point-charge system (q_i) with their respective coordinates (x_i, y_i, z_i) that interacts with interior of the box via the coulombic electrostatic potential

$$\hat{V} = \sum_{i=1}^m \frac{q_i}{\sqrt{(x-x_i)^2 + (y-y_i)^2 + (z-z_i)^2}}$$

The external perturbation matrix is evaluated over all k states as:

$$V_{ij} = \int_0^a \int_0^b \int_0^c \psi_i^* \hat{V} \psi_j dx dy dz$$

and the total Hamiltonian is obtained by adding the unperturbed PIB T_{ij}^0 to the molecular perturbation

$$H_{ij} = T_{ij}^0 + V_{ij}$$

Next, we solve the secular equation to first order using perturbation theory:

$$H_{ij} \cdot \bar{c}_j = E_j \bar{c}_j$$

and can obtain the energy eigenstates and the 1st order PIB wavefunction coefficients. In this case the 1st order perturbed wavefunctions, $\psi_{(x,y,z)}$, can be expressed in terms of perturbed wavefunction coefficients, \bar{c}_j and the unperturbed PIB ground-state wavefunctions $\psi_{(x,y,z)}^0$, via

$$\psi_{(x,y,z)} = \sum_j \bar{c}_j \cdot \psi_{(x,y,z)}^0$$

This expression along with the unperturbed PIB wavefunction expressions enables us to obtain the wavefunction probability density of both perturbed and unperturbed states, and the differences of these two quantities:

$$\rho_{\text{perturbed}} = \int_0^a \int_0^b \int_0^c (\bar{c}_j \cdot \psi_{(x,y,z)}^0)^2 dx dy dz$$

$$\rho_{\text{unperturbed}} = \int_0^a \int_0^b \int_0^c (\bar{c}_j^0 \cdot \psi_{(x,y,z)}^0)^2 dx dy dz$$

$$\rho_{\text{electron}} = \rho_{\text{perturbed}} - \rho_{\text{unperturbed}}$$

$$\rho_{\text{hole}} = \rho_{\text{unperturbed}} - \rho_{\text{perturbed}}$$

enables us to compute the induced CICs in the nanoparticle. The overall schematic of this approach can be summarized in Figure 1 of the paper, in which an initial system comprised of a single chiral adsorbate (R-Methylthiirane) adsorbed to a Au₁₄ nanoparticle substrate is (b) coarse grained to point-charges and allowed to interact via a coulombic electrostatic potential.

1.3. Calculation of Chiroptic Signatures in MPCs

In order to theoretically calculate properties related to optical activity, the primary quantity that we concern ourselves with is the rotational strength, R . This property can be computed quantum mechanically if the induced electric dipole and magnetic dipole transition elements are known. The electric dipole operator,

$$\hat{\mu} = \hat{x} + \hat{y} + \hat{z}$$

and the magnetic dipole moment operator,

$$\hat{m} = i\left[\hat{x}\frac{\partial}{\partial y} - \hat{y}\frac{\partial}{\partial x}\right] + i\left[\hat{y}\frac{\partial}{\partial z} - \hat{z}\frac{\partial}{\partial y}\right] + i\left[\hat{z}\frac{\partial}{\partial x} - \hat{x}\frac{\partial}{\partial z}\right]$$

are the critical operators that we will use to compute the electric and magnetic transition-dipole moment matrix elements according to

$$\begin{aligned}\bar{\mu}_{n0} &= \int \psi_n^* \hat{\mu} \psi_0 dxdydz \\ \bar{m}_{n0} &= \int \psi_n^* \hat{m} \psi_0 dxdydz\end{aligned}$$

These quantities will then give us our desired Rotational Strength, R_{n0} . Similarly one can obtain the oscillator strength, F_{n0} using the electric dipole moment transition elements, as explained in the paper. Using the rotational strength one can approximate a CD spectrum by using a gaussian envelope expression for the first several HOMO-LUMO transition element contributions (i.e. the most easily excitable transitions in the HOMO-LUMO gap), and ascribing the exponential decay of the gaussian envelopes by the experimental peak-width at half height.

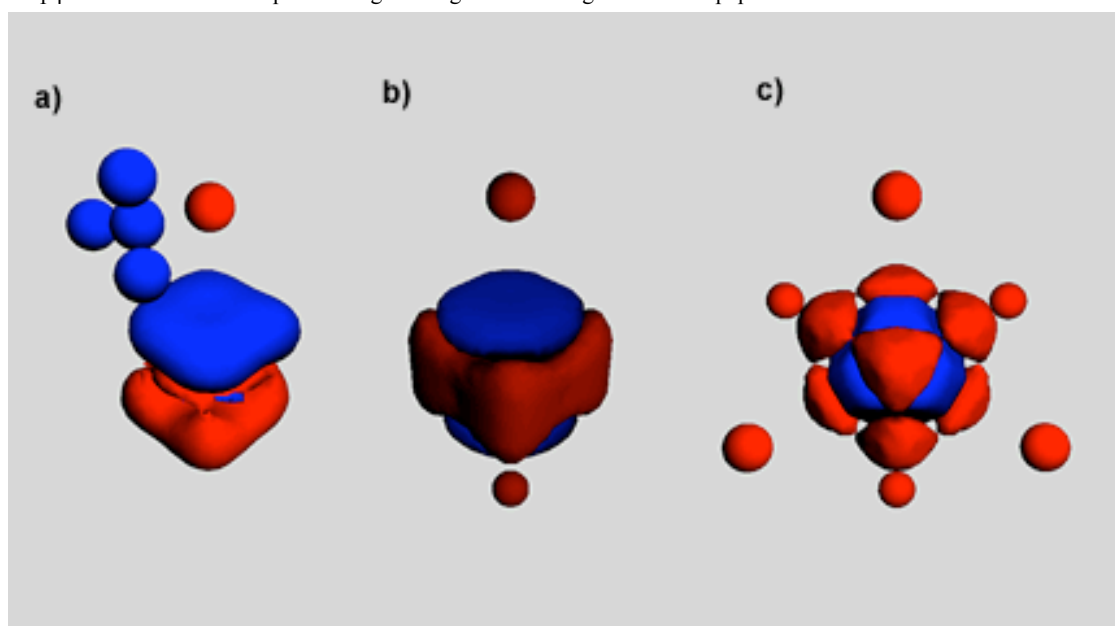
2.1. Generation of Gold nanoparticles and Adsorbates

All gold nanoparticle structures (i.e. Au cores) used in this study are based on the bulk gold lattice Fm-3m space group, cubic close-packed (ccp) structure (a=b=c=4.08 Angstrom).[8] The number of "particles" used in the CPPIB model for cores 1-4 are equal to the number of gold atoms present under the *ad hoc* assumption that each gold atom may contribute its outermost 6s¹ valence electron to the conduction band of the metal, hence making an n-particle in a box problem.

The adsorbates used in this study in conjunction with the aforementioned gold nanoparticle cores used to generate our theoretical CMPCs were (i) R-methylthiirane (MTI) and (ii) glutathione (SG). The mono-ligated and hexa-ligated CMPCs were geometry-optimized using the MMX force-field as implemented in Hyperchem 6.0, and were attached to the gold clusters (14, 28 atom core sizes).[2] The charges on the adsorbates are derived using a Mulliken population analysis in the semi-empirical quantum mechanical Extended-Huckel [1] framework with the nanoparticle present. The sulfur atoms of both types of ligands groups are assumed to attach to Au to make the adsorbate/Au core CMPCs, and so the separation between the thiol linker and Au was chosen to be 2.403 Angstrom based upon recent DFT calculations [9,b]) and positioned in the atop position above a face-centered gold atom in the cpp structure, unless otherwise indicated. Again, these are theoretically sound models of gold nanoparticle/adsorbate clusters chosen on their past performance, or in their ease of phenomenologically describing the problem at hand. In the case of the point-charge systems seen in Figure 2 of the paper, the charge were assigned to a single negative point charge based on the average value of methyl thiolate atom mulliken charges in the structures used (-0.8 e).

2.1.2 The Symmetric Perturbation (the optically inactive case)

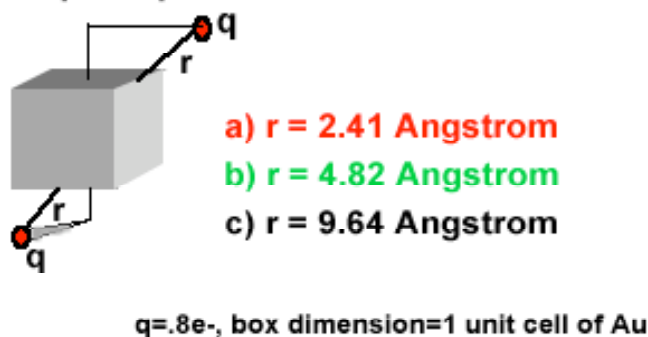
Included are several representative induced image charges for the achiral particle in a box, where point charge perturbations are placed in symmetric fashions around the box. The rotational strength for these configurations are zero, and the absorption spectra are identical to those observed in the chiral case with respect to surface coverage (i.e. 2 point charge chiral or achiral arrangements produces identical UV spectra on an identical core size.) The first case shows (a) methylthiolate (Methyl are blue point charges and red is negative charge of sulfur), then a coarse grained (b) “dimethyl” point charge set-up with point charges above and below the center of two faces on opposite sides. Finally (c) the 6 face centered point charge configuration, again showing symmetry in the induced image charges. The gold nanoparticle core is Au₁₄ as seen in the chiral point-charge arrangements in Figure 2 of the paper.



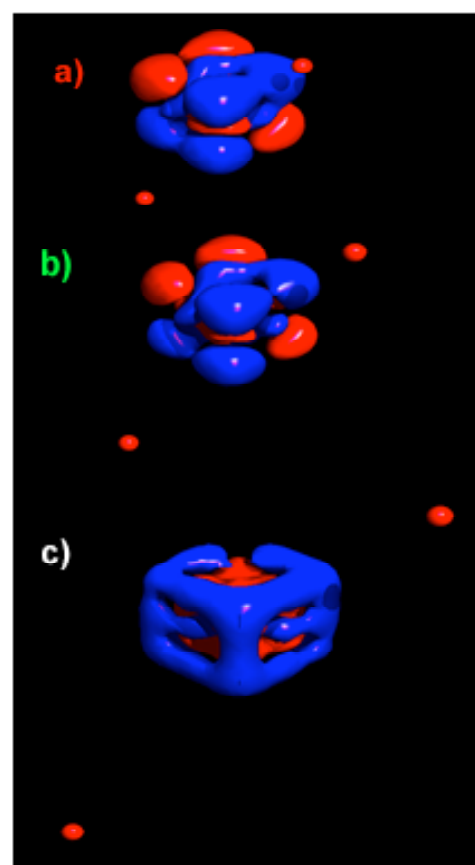
2.1.3 The Distance-Dependence of a Dissymmetric perturbation (Demonstration)

We demonstrate using (I) a 2 point charge model arranged in a dissymmetric pattern in the figure below (similar to that shown in the communication in Figure 2(a)) that the induced chiral image charge (shown in III below) changes as a function of separation distance, becoming more symmetric as the chiral perturbation is weakened by separating the distance of the chirally arranged perturbing point charges from the core. Similarly, we also demonstrate for the same separation distances the effects of (a) an initial given separation distance between the point charges and the core (b) doubling the distance and (c) quadrupling the separation distance and the resulting effect on the CD spectrum (Shown in (II) below.)

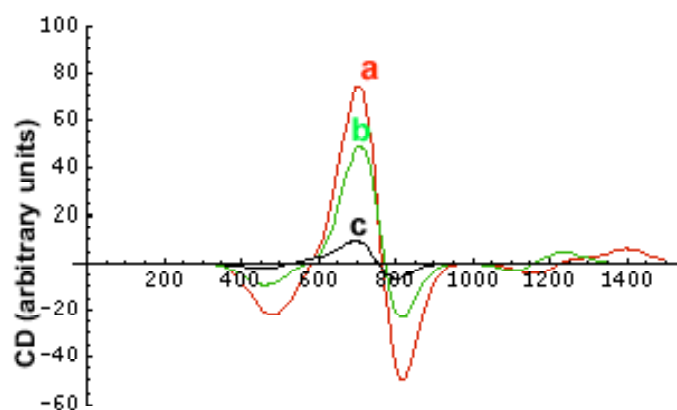
(I) 2 point-charge chiral adsorption pattern model



(III) Dist.-Dep. of image charge in core based on model (I)



(II) Dist.-dependent CD from model (I)



2.2. CIC calculation using Extended Huckel Theory

In the mixed model Extended Huckel approach, we perform a calculation on the gold nanocluster to obtain the unperturbed core wavefunction, and subsequently on the gold-nanocluster in the presence of the point-charge approximation of the adsorbate. These two calculations represent the unperturbed and perturbed states respectively. The correction of these classical charges to the diagonal elements of the Hamiltonian matrix may be written as:

$$\Delta H_{ii} = \alpha \sum_j \frac{Q_j}{R_{ij}}$$

and the off-diagonal elements of the Hamiltonian matrix are computed based on the corrected diagonal elements. In this equation, α is a scale factor for the classical-quantum interaction, m is the m th atomic orbital belonging to atom i , Q_j is a pure charge on atom j in the classical region, R_{ij} is the distance between atom i in the selected region and atom j in the unselected region, and the sum is over all atoms in the unselected region. The basis function used in this model is a STO-6G basis set, with p and d functions computed using Hyperchem 6.0 (Hypercube Inc.).

In order for us to compute the chiral image-charge, we perform a calculation on a bare core (Au₁₄ for instance) alone to obtain the atomic charges and our unperturbed core density. Then, we compute the charges on the admolecule placed in the adsorbed position in the presence of the precomputed gold charges using the mixed-model approach, however the core charges appear as perturbation terms to the Hamiltonian of the adsorbate. Subsequently, we compute the gold core in the presence of the admolecule charges, which represents our perturbed gold density. A separate Tcl script was created to extract difference density maps between perturbed and unperturbed nanoparticles based on their AO coefficients. The purpose of these calculations is entirely qualitative for comparison of electron density distribution maps in perturbed nanoclusters. Likewise, the EHT mixed model methodology was used to obtain the point-charges used in the CPPIB model. The representative results of such a calculation are shown in Figure 4(a) of the paper. One should also note that the size of the difference surface is scaled up so that the symmetry of the perturbation may be observed: regardless of theory used these are weak perturbations of symmetry to the core, typically resulting in charge polarization displacements of 1×10^{-5} elementary charge units.

2.3. CD spectra using TD-RI-DFT

The same coordinates for the Au₁₄(R-Methylthiirane) used for the CPPIB model to which comparisons are made are used in the DFT calculations presented here. The calculations were performed within Turbomole 5.6 using TD-DFT with the RI approximation with the non-hybrid gradient-corrected BP86 functional and the Au pseudopotential within a single-excitation RPA calculation that includes the first 10 single excitations.[10-15] In addition to computing the CD spectrum of the aforementioned system with an all-atom description (as seen in Figure 5 a) the admolecule was represented as point-charges as used in the CPPIB and EHT models to validate the method of coarse-graining (figure 5, b). The resulting CD was developed in a manner analogous to the description in the CPPIB treatment (a gaussian envelope approximation). However, it may be noted that another possible source of discrepancy between the observed band height (i.e. Rotational Strength) is due to the use of EHT charges in Figure 5b, and in the case of the CPPIB model a potential lack of description for charge transfer between admolecule and core. Nonetheless, the same sign, and spectral region are observed in all three cases. The region of the induced CD spectral bands is qualitatively in agreement with experiment, although a more practical application would be to all solvent accessible conformations and subsequent Boltzmann weighting of the CD spectra, which may improve calculations of chiral image-charges or CD spectra in the chirally-perturbed PIB model in addition to the EHT, or DFT approach.

To the best of our knowledge there have been no published theoretical calculations of chiral image-charge densities or induced CD spectra in chiral monolayer protected clusters using any of the theoretical approaches used in this study to

date. The concepts herein are completely novel, and general, and probe the effects of external dissymmetrically placed chiral or achiral ligands on achiral core structures, though they may be used more generally to probe external perturbations to an electronic structure of any kind of symmetry, or any type of metal provided that basis sets have been developed (in the case of DFT and EHT) or more formally in the chirally-perturbed model, provided that the experimental system behaves in a jellium fashion.

- [1] R. Hoffmann, *J. Chem. Phys.*, **1963**, *39*, 1397.
[2] **HyperChem 6.0** program, Hypercube Inc. Gainesville, USA
[3] Ph. Avouris, I.-W. Lyo, R.E. Walkup, *J. Vac. Sci. Technol. B* **1994**, *12*, 1447-1455.
[4] M. Vos, E. Weigold, *J. Electron Spectrosc. Relat. Phenom.* **2002**, *123*, 333-344.
[5] G. Mills, B. Wang, W. Ho, H. Metiu, *J. Chem. Phys.* **2004**, *120*, 7738-7740.
[6] J. Zheng, C.W. Zhang, R.M. Dickson, *Phys Rev Lett.* **2004**, *93*, Art. No. 077402.
[7] **gridMathematica** v. 5.0, Wolfram Inc. **2005**
[8] a) <http://www.webelements.com/webelements/elements/text/Au/xtal-vr.html> b) A. Maeland and T.B. Flanagan *Can. J. Phys.* **1964** *42* 2364
[9] a) Y. Negishi, T. Tsukuda, *J. Am. Chem. Soc.* **2003**, *125*, 4046-4047. (b) Y. Negishi, Y. Takasugi, S. Sato, H. Yao, K. Kimura, T. Tsukuda, *J. Am. Chem. Soc.* **2004**, *126*, 6518-6519. (c) K. Nobusada, *J. Phys. Chem. B* **2004**, *108*, 11904-11908. (d) J.A. Larsson, M. Nolan, J.C. Greer, *J. Phys. Chem. B* **2002**, *106*, 5931-5937.
[10] S. Grimme, J. Harren, A. Sobanski and F. Vogtle *Eur. J. Org. Chem.* **1998** 1491.
[11] K. Eichkorn, O. Treutler, H. Öhm, M. Häser, R. Ahlrichs, *Chem. Phys. Lett.* **1995**, *98*, 283-290.
[12] S. Grimme, F. Furche, R. Ahlrichs, *Chem. Phys. Lett.* **2002**, *361*, 321-328.
[13] R. Ahlrichs, M. Bär, H.-P. Baron, R. Bauernschmitt, S. Böcker, M. Ehrig, K. Eichkorn, S. Elliott, F. Furche, F. Haase, M. Häser, H. Horn, C. Huber, U. Huniar, M. Kattannek, C. Kolmel, M. Kollwitz, K. May, C. Ochsenfeld, H. Öhm, A. Schäfer, U. Schneider, O. Treutler, M. von Arnim, F. Weigend, P. Weis, H. Weiss, *Turbomole (version 5.6)*; Universität Karlsruhe: Karlsruhe, Germany, 2002.
[14] a) A.D. Becke, *Phys. Rev. A* **1988**, *38*, 3098-3100. b) J.P. Perdew, *Phys. Rev. B* **1986**, *33*, 8822-8824.
[15] K. Eichkorn, F. Weigend, O. Treutler, R. Ahlrichs, *Theor. Chem. Acc.* **1997**, *97*, 119-124.